Search for Spectral Irregularities due to Photon-Axionlike-Particle Oscillations with the Fermi Large Area Telescope

(Article begins on next page)
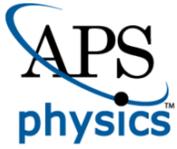
16 October 2023

Search for Spectral Irregularities due to Photon–Axionlike-Particle Oscillations with the Fermi Large Area Telescope

M. Ajello *et al.* (The Fermi-LAT Collaboration)

Search for spectral irregularities due to photon-axion-like particle oscillations with the *Fermi* Large Area Telescope

M. Ajello,[1] A. Albert,[2] B. Anderson,[3,4] L. Baldini,[5,2] G. Barbiellini,[6,7] D. Bastieri,[8,9]

R. Bellazzini,[10] E. Bissaldi,[11] R. D. Blandford,[2] E. D. Bloom,[2] R. Bonino,[12,13]

E. Bottacini,[2] J. Bregeon,[14] P. Bruel,[15] R. Buehler,[16] G. A. Caliandro,[2,17] R. A. Cameron,[2]

M. Caragiulo,[18,11] P. A. Caraveo,[19] C. Cecchi,[20,21] A. Chekhtman,[22] S. Ciprini,[23,20]

J. Cohen-Tanugi,[14] J. Conrad,[3,4,24,*] F. Costanza,[11] F. D'Ammando,[25,26] A. de Angelis,[27]

F. de Palma,[11,28] R. Desiante,[29,12] M. Di Mauro,[2] L. Di Venere,[18,11] A. Domínguez,[1]

P. S. Drell,[2] C. Favuzzi,[18,11] W. B. Focke,[2] A. Franckowiak,[2] Y. Fukazawa,[30] S. Funk,[31]

P. Fusco,[18,11] F. Gargano,[11] D. Gasparrini,[23,20] N. Giglietto,[18,11] T. Glanzman,[2]

G. Godfrey,[2] S. Guiriec,[32,33] D. Horan,[15] G. Jóhannesson,[34] M. Katsuragawa,[35]

S. Kensei,[30] M. Kuss,[10] S. Larsson,[36,4] L. Latronico,[12] J. Li,[37] L. Li,[36,4] F. Longo,[6,7]

F. Loparco,[18,11] P. Lubrano,[20] G. M. Madejski,[2] S. Maldera,[12] A. Manfreda,[10]

M. Mayer,[16] M. N. Mazziotta,[11] M. Meyer,[3,4,†] P. F. Michelson,[2] N. Mirabal,[32,33]

T. Mizuno,[38] M. E. Monzani,[2] A. Morselli,[39] I. V. Moskalenko,[2] S. Murgia,[40]

M. Negro,[12,13] E. Nuss,[14] C. Okada,[30] E. Orlando,[2] J. F. Ormes,[41] D. Paneque,[42,2]

J. S. Perkins,[32] M. Pesce-Rollins,[10,2] F. Piron,[14] G. Pivato,[10] T. A. Porter,[2]

S. Rainò,[18,11] R. Rando,[8,9] M. Razzano,[10,43] A. Reimer,[44,2] M. Sánchez-Conde,[4,3,‡]

C. Sgrò,[10] D. Simone,[11] E. J. Siskind,[45] F. Spada,[10] G. Spandre,[10] P. Spinelli,[18,11]

H. Takahashi,[30] J. B. Thayer,[2] D. F. Torres,[37,46] G. Tosti,[20,21] E. Troja,[32,47]

Y. Uchiyama,[48] K. S. Wood,[49] M. Wood,[2] G. Zaharijas,[50,51] and S. Zimmer[3,4]

[1]*Department of Physics and Astronomy, Clemson University,*

Kinard Lab of Physics, Clemson, SC 29634-0978, USA

[2]*W. W. Hansen Experimental Physics Laboratory,*

Kavli Institute for Particle Astrophysics and Cosmology,

Department of Physics and SLAC National Accelerator Laboratory,

Stanford University, Stanford, CA 94305, USA

[3]*Department of Physics, Stockholm University,*

AlbaNova, SE-106 91 Stockholm, Sweden

[4]*The Oskar Klein Centre for Cosmoparticle Physics,*

AlbaNova, SE-106 91 Stockholm, Sweden

[5]Università di Pisa and Istituto Nazionale di Fisica Nucleare,

Sezione di Pisa I-56127 Pisa, Italy

[6]Istituto Nazionale di Fisica Nucleare,

Sezione di Trieste, I-34127 Trieste, Italy

[7]Dipartimento di Fisica, Università di Trieste, I-34127 Trieste, Italy

[8]Istituto Nazionale di Fisica Nucleare,

Sezione di Padova, I-35131 Padova, Italy

[9]Dipartimento di Fisica e Astronomia "G. Galilei",

Università di Padova, I-35131 Padova, Italy

[10]Istituto Nazionale di Fisica Nucleare,

Sezione di Pisa, I-56127 Pisa, Italy

[11]Istituto Nazionale di Fisica Nucleare,

Sezione di Bari, I-70126 Bari, Italy

[12]Istituto Nazionale di Fisica Nucleare,

Sezione di Torino, I-10125 Torino, Italy

[13]Dipartimento di Fisica Generale "Amadeo Avogadro" ,

Università degli Studi di Torino, I-10125 Torino, Italy

[14]Laboratoire Univers et Particules de Montpellier,

Université Montpellier, CNRS/IN2P3, Montpellier, France

[15]Laboratoire Leprince-Ringuet, École polytechnique, CNRS/IN2P3, Palaiseau, France

[16]Deutsches Elektronen Synchrotron DESY, D-15738 Zeuthen, Germany

[17]Consorzio Interuniversitario per la Fisica Spaziale (CIFS), I-10133 Torino, Italy

[18]Dipartimento di Fisica "M. Merlin" dell'Università

e del Politecnico di Bari, I-70126 Bari, Italy

[19]INAF-Istituto di Astrofisica Spaziale e Fisica Cosmica, I-20133 Milano, Italy

[20]Istituto Nazionale di Fisica Nucleare,

Sezione di Perugia, I-06123 Perugia, Italy

[21]Dipartimento di Fisica, Università degli Studi di Perugia, I-06123 Perugia, Italy

[22]College of Science, George Mason University, Fairfax, VA 22030,

resident at Naval Research Laboratory, Washington, DC 20375, USA

[23]Agenzia Spaziale Italiana (ASI) Science Data Center, I-00133 Roma, Italy

[24] *Wallenberg Academy Fellow*

[25] *INAF Istituto di Radioastronomia, I-40129 Bologna, Italy*

[26] *Dipartimento di Astronomia, Università di Bologna, I-40127 Bologna, Italy*

[27] *Dipartimento di Fisica, Università di Udine and Istituto Nazionale di Fisica Nucleare,*

Sezione di Trieste, Gruppo Collegato di Udine, I-33100 Udine

[28] *Università Telematica Pegaso, Piazza Trieste e Trento, 48, I-80132 Napoli, Italy*

[29] *Università di Udine, I-33100 Udine, Italy*

[30] *Department of Physical Sciences, Hiroshima University,*

Higashi-Hiroshima, Hiroshima 739-8526, Japan

[31] *Erlangen Centre for Astroparticle Physics, D-91058 Erlangen, Germany*

[32] *NASA Goddard Space Flight Center, Greenbelt, MD 20771, USA*

[33] *NASA Postdoctoral Program Fellow, USA*

[34] *Science Institute, University of Iceland, IS-107 Reykjavik, Iceland*

[35] *Institute of Space and Astronautical Science,*

Japan Aerospace Exploration Agency, 3-1-1 Yoshinodai,

Chuo-ku, Sagamihara, Kanagawa 252-5210, Japan

[36] *Department of Physics, KTH Royal Institute of Technology,*

AlbaNova, SE-106 91 Stockholm, Sweden

[37] *Institute of Space Sciences (IEEC-CSIC),*

Campus UAB, E-08193 Barcelona, Spain

[38] *Hiroshima Astrophysical Science Center, Hiroshima University,*

Higashi-Hiroshima, Hiroshima 739-8526, Japan

[39] *Istituto Nazionale di Fisica Nucleare,*

Sezione di Roma "Tor Vergata", I-00133 Roma, Italy

[40] *Center for Cosmology, Physics and Astronomy Department,*

University of California, Irvine, CA 92697-2575, USA

[41] *Department of Physics and Astronomy,*

University of Denver, Denver, CO 80208, USA

[42] *Max-Planck-Institut für Physik, D-80805 München, Germany*

[43] *Funded by contract FIRB-2012-RBFR12PM1F from the*

Italian Ministry of Education, University and Research (MIUR)

[44]*Institut für Astro- und Teilchenphysik and Institut für Theoretische Physik,*

Leopold-Franzens-Universität Innsbruck, A-6020 Innsbruck, Austria

[45]*NYCB Real-Time Computing Inc.,*

Lattingtown, NY 11560-1025, USA

[46]*Institució Catalana de Recerca i Estudis Avançats (ICREA), Barcelona, Spain*

[47]*Department of Physics and Department of Astronomy,*

University of Maryland, College Park, MD 20742, USA

[48]*Department of Physics, 3-34-1 Nishi-Ikebukuro,*

Toshima-ku, Tokyo 171-8501, Japan

[49]*Space Science Division, Naval Research Laboratory, Washington, DC 20375-5352, USA*

[50]*Istituto Nazionale di Fisica Nucleare, Sezione di Trieste,*

and Università di Trieste, I-34127 Trieste, Italy

[51]*Laboratory for Astroparticle Physics, University of Nova Gorica,*

Vipavska 13, SI-5000 Nova Gorica, Slovenia

(Dated: April 6, 2016)

Abstract

We report on the search for spectral irregularities induced by oscillations between photons and axion-like particles (ALPs) in the γ-ray spectrum of NGC 1275, the central galaxy of the Perseus cluster. Using six years of *Fermi* Large Area Telescope data, we find no evidence for ALPs and exclude couplings above $5 \times 10^{-12}\,\mathrm{GeV}^{-1}$ for ALP masses $0.5 \lesssim m_a \lesssim 5\,\mathrm{neV}$ at $95\,\%$ confidence. The limits are competitive with the sensitivity of planned laboratory experiments, and, together with other bounds, strongly constrain the possibility that ALPs can reduce the γ-ray opacity of the Universe.

INTRODUCTION

Axions and axion-like particles (ALPs) are predicted by a variety of extensions of the Standard Model [1–6]. If produced non-thermally in the early Universe, these particles may account for all or a significant fraction of the cold dark matter (DM) [e.g. 7–9], and could be detected through their coupling to photons in magnetic fields [10]. While the axion mass is proportional to its coupling to photons, these two parameters are independent in the case of ALPs.

Photon-ALP interactions could leave an imprint on γ-ray spectra, provided that the ALP mass is sufficiently small, $m_a \lesssim \mu$eV. Above a critical energy E_{crit} photon-ALP mixing becomes maximal, leading to a reduction of the photon flux [11, 12]. Around E_{crit} this is accompanied by spectral irregularities that depend on the strength and morphology of the magnetic field [13]. Photon-ALP conversions could also reduce the opacity of the Universe caused by pair production of γ rays with photons of the extragalactic background light (EBL) [14]. Evidence exists that the γ-ray absorption is indeed lower than expected from state-of-the-art EBL models [15–18], and ALPs have been used to explain these observations [19–22] (see, however, [23, 24]).

Sources embedded in galaxy clusters are promising to search for ALPs due to the strong magnetic fields extending over large spatial scales in these systems. For example, the absence of irregularities above $200\,\mathrm{GeV}$ in the spectrum of the blazar PKS 2155-304, associated with a poor galaxy cluster, has been used to constrain the photon-ALP coupling [25]. Here, we focus on the search for irregularities in the spectrum of the radio galaxy NGC 1275 with the *Fermi* Large Area Telescope (LAT). NGC 1275 is the most favorable target since it is a bright γ-ray emitter detected with a significance exceeding $100\,\sigma$ in the third *Fermi*-LAT source catalog (3FGL) [26]. Its broadband emission can be explained with synchrotron-self Compton models, which predict a smooth γ-ray spectrum [28, 29]. It is located at the center of the Perseus cool-core cluster for which rotation measures (RMs) suggest a high central magnetic field [30].

Our analysis makes use of the newest `Pass 8` event-level analysis for LAT data. Compared to previous Passes, `Pass 8` has an improved angular resolution, a broader energy range, larger effective area, as well as reduced uncertainties in the instrumental response functions (IRFs) [31].

LAT DATA SELECTION

141   We make use of six years of LAT data taken between 2008-08-04 and 2014-08-04 in the
142 energy range from 100 MeV to 500 GeV. For lower energies, the effective area decreases
143 rapidly and the energy dispersion increases. At energies above 500 GeV we do not expect
144 sufficient photon statistics [32]. We only consider events that arrive at a zenith angle $\theta_z < 90°$
145 in order to minimize the contribution of γ rays from the Earth limb. Time intervals that
146 correspond to bright solar flares and γ-ray bursts are excluded. We extract γ-ray like
147 events within a $10° \times 10°$ region of interest (ROI) centered at the position of NGC 1275:
148 $\alpha_{2000} = 3^\mathrm{h}19^\mathrm{m}49.9^\mathrm{s}$, $\delta_{2000} = +41°30^\mathrm{m}49.2^\mathrm{s}$ [26].

149   Events passing the `Pass 8 P8R2_SOURCE` selection cuts are analyzed using the `P8R2_SOURCE_V6`
150 IRFs.[1] An innovation of the `Pass 8` IRFs is the possibility to subdivide an event class into
151 event types according to the quality of the angular or energy reconstruction (PSF and
152 EDISP event types, respectively). In this analysis we will use the EDISP types to maximize
153 our sensitivity to spectral irregularities. Events are classified into one of four types ranging
154 from EDISP0 to EDISP3, that denote the quality of the energy reconstruction from worst to
155 best. All EDISP event types have a similar number of events in each logarithmic energy bin
156 and are mutually exclusive. The energy dispersion matrices are given in the Supplemental
157 Material [27].

158 **PHOTON-ALP OSCILLATIONS**

159   Following [16, 33, 34], we derive the probability $P_{\gamma\gamma}$ for a final state photon in the photon-
160 ALP beam as a function of energy for an initially un-polarized photon beam (see the Sup-
161 plemental Material). We expect the irregularities to occur around a critical energy [35],

$$E_{\mathrm{crit}} \sim 2.5\,\mathrm{GeV}\,\frac{|m_{a,\mathrm{neV}}^2 - \omega_{\mathrm{pl,neV}}^2|}{g_{11}B_{\mu\mathrm{G}}}, \tag{1}$$

162 with ALP mass $m_{a,\mathrm{neV}}$ and plasma frequency $\omega_{\mathrm{pl,neV}}$ in units of neV, coupling constant
163 $g_{11} = g_{a\gamma}/10^{-11}\mathrm{GeV}^{-1}$, and magnetic field $B_{\mu\mathrm{G}} = B/1\,\mu\mathrm{G}$. We include photon-ALP mixing
164 in the intra-cluster and Galactic magnetic fields. The B field of the Milky Way is modeled
165 with the coherent component of the model described in [36]. We do not include its turbulent

---

[1] http://www.slac.stanford.edu/exp/glast/groups/canda/lat_Performance.htm

component, as the scales on which the turbulence occurs are usually smaller than the photon-ALP oscillation length. The turbulent intra-cluster B field is described below. Absorption of γ rays by the EBL is taken into account through the model of [37]. We neglect any oscillations in the intergalactic magnetic field (IGMF). With current upper limits on the IGMF strength of $\lesssim 10^{-9}\,\mathrm{G}$ and on the photon-ALP coupling, $g_{11} < 6.6$ [38], we find that $E_{\mathrm{crit}} \lesssim 100\,\mathrm{GeV}$ only for $m_{a,\mathrm{neV}} \lesssim 0.5$. For such low masses, g_{11} is further constrained below 0.6 from the non-observation of γ rays from SN1987A [39]. Given this small coupling and the comparatively short distance to NGC 1275 (redshift $z = 0.017559$), no strong irregularities should be induced by mixing in the IGMF.

Intra-cluster magnetic field

Faraday RM observations and magneto-hydrodynamic simulations suggest that the magnetic field in galaxy clusters is turbulent and that its strength follows the electron density $n_e(r)$ of the intra-cluster medium (ICM), $B(r) = B_0(n_e(r)/n_e(r=0))^\eta$ [40–42]. We model the turbulent component as a divergence-free homogeneous isotropic field with Gaussian turbulence with zero mean and a variance σ_B [34]. The energy density follows a power law $M(k) \propto k^q$ in wave numbers k. It is non-zero only between the minimum and maximum turbulence scales $k_L = 2\pi/\Lambda_{\mathrm{max}}$ and $k_H = 2\pi/\Lambda_{\mathrm{min}}$.

For the Perseus cluster, we use $n_e(r)$ derived from X-ray observations (Eq. (4) in [43]) within the inner $r_{\mathrm{max}} = 500\,\mathrm{kpc}$. Beyond this radius, we conservatively assume a zero magnetic field. RMs currently only probe the innermost region (tens of pc) around NGC 1275. The observations lead to an estimated central magnetic field of $25\,\mu\mathrm{G}$ [30]. An independent lower limit of $B_0 \gtrsim 2-13\,\mu\mathrm{G}$ for $0.3 \leq \eta \leq 0.7$ has been derived from MAGIC observations of the Perseus cluster [44]. These results motivate our assumptions for $\sigma_B = 10\,\mu\mathrm{G}$ and $\eta = 0.5$, which are also in line with observations of other cool-core clusters [e.g. 45, 46].

For the turbulence spectrum, we assume values derived from RMs of the cool-core cluster A 2199 [46], which has a comparable number of member galaxies. The fiducial parameter choices are summarized in Tab. I.

7

Parameter	Value
σ_B	$10\,\mu\mathrm{G}$
r_{max}	$500\,\mathrm{kpc}$
η	0.5
q	-2.8
Λ_{min}	$0.7\,\mathrm{kpc}$
Λ_{max}	$35\,\mathrm{kpc}$

TABLE I. Fiducial model parameters for the intra-cluster magnetic field in Perseus.

DATA ANALYSIS

We perform a binned Poisson likelihood analysis, similar to the DM signal search from dwarf spheroidal galaxies [47, 48]. Events are binned into $10°\times10°$ sky maps with a resolution of $0.2°$ per pixel. The width of the logarithmically spaced energy bins is chosen to be $30\,\%$ of the median energy resolution of each EDISP event type (see the Supplemental Material for details). This results in 39, 67, 94, and 145 energy bins for EDISP0-3, respectively. We have tested with simulations that bin sizes below $40\,\%$ of the median energy resolution do not affect the results.

For each event type, we perform a fit over the entire energy range and ROI for all source parameters (nuisance parameters $\boldsymbol{\theta}_i$) using *gtlike* included in the *Fermi*-LAT *Science Tools* version v10r01p01.[2] We include all point sources listed in the 3FGL within $15°$ from the ROI center. The diffuse backgrounds are modeled with templates for the Galactic and the isotropic extragalactic γ-ray emission.[3] The energy dispersion is taken into account in the fitting of the point sources whereas it is already accounted for in the the data-driven derivation of the diffuse templates. Normalizations of the diffuse sources and point sources within $8°$ from the ROI center are left free to vary. All spectral indices of the point sources within $4°$ are also free parameters. The time-averaged spectrum of NGC 1275 is modeled with a logarithmic (log) parabola, $F(E) = N(E/E_0)^{-(\alpha+\beta\ln(E/E_0))}$, where E_0 is fixed to 530 MeV [26].

Under the assumption that the profiled nuisance parameters do not change when con-

---

[2] http://fermi.gsfc.nasa.gov/ssc/data/analysis/

[3] http://fermi.gsfc.nasa.gov/ssc/data/access/lat/BackgroundModels.html

8

sidering each bin separately [47], we extract the likelihood in each reconstructed energy bin k', $\mathcal{L}(\mu_{ik'}, \boldsymbol{\theta}_i | D_{ik'})$ as a function of expected counts $\mu_{ik'}$ of NGC 1275, and observed counts $D_{ik'}$. For NGC 1275 a power law with fixed spectral index $\Gamma = 2$ is now assumed in each bin. For each tested value of $\mu_{ik'}$ we re-optimize the normalization of the spectrum of the radio galaxy IC 310 which has an angular separation of $\sim 0.6°$ from NGC 1275.

Under the ALP hypothesis, characterized by $P_{\gamma\gamma} \equiv P_{\gamma\gamma}(E, m_a, g_{a\gamma}, \mathbf{B}_j)$ for one random turbulent B-field realization $\mathbf{B}_j$, the expected number of photons is calculated through

$$\mu_{ik'} = \sum_k \mathcal{D}^i_{kk'} \int_{\Delta E_k} \mathrm{d}E \, P_{\gamma\gamma} F(E) \mathcal{E}^i(E), \tag{2}$$

where the integration runs over the true energy bin ΔE_k, $\mathcal{E}^i$ is the exposure, and $\mathcal{D}^i_{kk'}$ is the energy dispersion for event type EDISPi. Under the null hypothesis, $P_{\gamma\gamma}$ reduces to the EBL attenuation. The parameters of the intrinsic source spectrum $F(E)$, N, α, and β, are further nuisance parameters. For each tested ALP parameter and magnetic field, we determine these parameters by profiling the joint likelihood of all energy bins k'

$$\mathcal{L}_i(\boldsymbol{\mu}, \boldsymbol{\theta} | \mathbf{D}) \equiv \prod_{k'} \mathcal{L}(\mu_{ik'}, \boldsymbol{\theta}_i | D_{ik'}), \tag{3}$$

for each event type separately, using the pre-computed likelihood curves $\mathcal{L}(\mu_{ik'}, \boldsymbol{\theta}_i | D_{ik'})$. In this way, we treat each event type selection as an independent measurement.[4] The bin-by-bin likelihood curves for the EDISP3 event type are shown in Fig. 1 together with the best-fit spectra.

We simulate $N_B = 500$ random realizations of the turbulent field $\mathbf{B}_j$, $j = 1, \ldots, N_B$. The dependence of the likelihood on the realizations is not easily parametrizable and we cannot assume that the simulations map the space of possible realizations. Therefore, instead of profiling, we sort the B-field realizations for each tested $(m_a, g_{a\gamma})$ pair by increasing values of the product over the likelihoods $\mathcal{L}_i$ and use the realization that corresponds to the $Q_B = 0.95$ quantile of the likelihood distribution (profiling would correspond to $Q_B = 1$). We will denote this realization as $\mathbf{B}_{95}$ and the corresponding expected counts with $\boldsymbol{\mu}_{95}$. Note that $\mathbf{B}_{95}$ might be different for different ALP parameters, so that $\mathbf{B}_{95} \equiv \mathbf{B}_{95}(m_a, g_{a\gamma})$.

---

[4] This procedure will result in different best-fit estimators for the source parameters for each event type. In this way, it is possible to speed up the optimization considerably. We have verified that our results do not change when the parameters of NGC 1275 are tied over the event types.
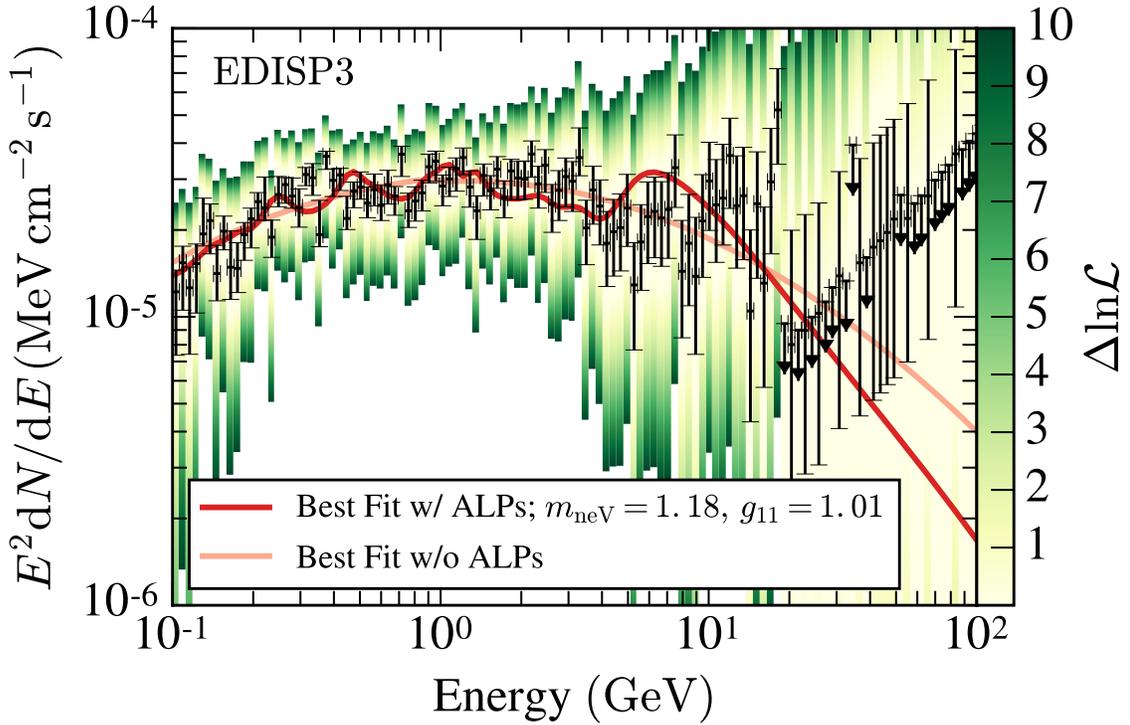
FIG. 1. The likelihood curves (shown in color) for the EDISP3 event type. $\Delta \ln \mathcal{L} = 0$ corresponds to the maximum likelihood in each bin (black points). The error bars indicate an increase of the likelihood by $2\Delta \ln \mathcal{L} = 1$. The best-fit spectrum of the joint likelihood without an ALP (with an ALP with $m_{\mathrm{neV}} = 1.2$ and $g_{11} = 1$) is shown as a light (dark) red solid line.

Similar to [49], we evaluate the ALP hypothesis with a likelihood ratio test. The test statistic (TS) for the ALP hypothesis is calculated from the joint likelihood of all event types:

$$\mathrm{TS} = -2 \sum_{i} \ln \left(\frac{\mathcal{L}_i(\boldsymbol{\mu}_0, \hat{\hat{\boldsymbol{\theta}}}|\mathbf{D})}{\mathcal{L}_i(\hat{\boldsymbol{\mu}}_{95}, \hat{\boldsymbol{\theta}}|\mathbf{D})} \right), \tag{4}$$

where $\boldsymbol{\mu}_0$ are the expected counts for the null (no ALP) hypothesis with maximized nuisance parameters $\hat{\hat{\boldsymbol{\theta}}} \equiv \hat{\boldsymbol{\theta}}(\boldsymbol{\mu}_0)$ and $\hat{\boldsymbol{\mu}}_{95}$ are the expected counts under the ALP hypothesis that, together with $\hat{\boldsymbol{\theta}}$, maximize the likelihoods of each event type. We test ALP parameters on a logarithmic $(m_a, g_{a\gamma})$ grid with (19×12) steps where $0.07 \leq m_{a,\mathrm{neV}} \leq 100$ and $0.1 \leq g_{11} \leq 7$. The mass range is chosen such that E_{crit} falls into the analyzed energy range whereas the maximum coupling is motivated by the bound found in [38]. For the lower bound, the

246 amplitude of the irregularities is too small to be detectable.

247   In order to convert the TS value into a significance, we need to know the underlying
248 probability distribution. We derive the null distribution from Monte-Carlo simulations and
249 from it the threshold TS value, $\mathrm{TS_{thr}}$, for which we can reject the null hypothesis (see the
250 Supplemental Material for details). For a rejection of the no-ALP hypothesis at a $3\,\sigma$ (global)
251 significance level, we find that $\mathrm{TS} > \mathrm{TS_{thr}} = 33.1$.

RESULTS

253   The best-fit ALP parameters are found at $m_{\mathrm{neV}} = 44.6$ and $g_{11} = 4.76$ with $\mathrm{TS} =$
254 $10.40 < \mathrm{TS_{thr}}$, and hence the best fit with ALPs is not significantly preferred over the null
255 hypothesis. We set upper limits by stepping over the ALP parameters and calculating the
256 difference $\lambda(m_a, g_{a\gamma})$ between the log-likelihood values for each pair m_a, $g_{a\gamma}$ and the best fit.
257 ALP parameters are excluded with $95\,\%$ confidence if $\lambda > \lambda_{\mathrm{thr}} = 22.8$. The threshold value
258 λ_{thr} is calculated under the assumption that the probability distribution of the alternative
259 hypothesis follows the null distribution. We have tested this assumption with simulations
260 and found that this choice results in over coverage for ALP parameters causing the strongest
261 irregularities, thus yielding conservative limits.

262   The excluded parameter space is shown in the left panel of Fig. 2 (black shaded region).
263 Photon-ALP couplings are ruled out between $0.5 \lesssim g_{11} \lesssim 3$ for $0.5 \lesssim m_{a,\mathrm{neV}} \lesssim 5$ and $g_{11} \gtrsim 1$
264 for $5 \lesssim m_{a,\mathrm{neV}} \lesssim 10$. At high masses, the limits run almost parallel to the lines of constant
265 E_{crit} (shown as dotted lines for $B_{\mu\mathrm{G}} = 10$). For lower masses, ALP couplings along the
266 $E_{\mathrm{crit}} = 1\,\mathrm{GeV}$ line with $1.3 \lesssim g_{11} \lesssim 4$ are not excluded. Around this "hole"-like feature,
267 $P_{\gamma\gamma}$ exhibits rapid fluctuations for almost the entire *Fermi*-LAT energy range. Given the
268 Poisson noise in the data, these ALP parameters cannot be excluded. We stress that the
269 fit with ALPs is not preferred over the null hypothesis. For masses below $m_{a,\mathrm{neV}} = 0.5$,
270 irregularities still enter the *Fermi*-LAT energy range allowing to exclude ALP parameters.

271   The observed limits agree well with the expected exclusion region derived from Monte-
272 Carlo simulations (shaded regions). The "hole" feature is not visible in the expected limits
273 but occurs in certain Monte-Carlo realizations (an example is given in the Supplemental
274 Material). In $5\,\%$ of the simulations (yellow shaded region), ALP parameters are excluded
275 for which the $E_{\mathrm{crit}} > 100\,\mathrm{GeV}$. This is expected since we have derived λ_{thr} from the null

distribution where for $5\,\%$ of the simulations one finds $\mathrm{TS} > \lambda_{\mathrm{thr}}$. The parameters for which we could detect an ALP signal at a $2\,\sigma$ level agree well with the observed limits (gray hatched region; see the Supplemental Material for details).

The results are subject to systematic uncertainties related to the analysis and magnetic field parameters. Concerning the analysis, changing the energy dispersion has the strongest effect on the limits. If we conservatively broaden the energy dispersion by $20\,\%$ the area of the tested ALP parameter grid with $\lambda > 22.8$ decreases by $25\,\%$. All other tested effects related to the analysis change the limits at most by $\sim 4\,\%$. Concerning the choice of B-field parameters, neither the strength, the power spectrum, nor the dependence on the electron density of the magnetic field are well established for Perseus. Therefore, the full analysis is repeated for a magnetic-field strength of $\sigma_B = 20\,\mu\mathrm{G}$, for a Kolmogorov-type turbulence spectrum, $q = -11/3$ (as found in the cool-core cluster Hydra A, [e.g. 45]), and by conservatively assuming that the magnetic field is zero beyond $r_{\mathrm{max}} = 100\,\mathrm{kpc}$. Increasing σ_B increases the excluded area by $43\,\%$. In comparison, the other tested parameters have a subdominant effect of maximally $16\,\%$. The dependence of the limits on the particular choice of the EBL model is negligible due to the relative proximity of $\mathrm{NGC\,1275}$ ($z = 0.017559$). The absorption is maximally $\sim 8\,\%$ at $500\,\mathrm{GeV}$ with significantly smaller relative differences for a number of EBL models [37, 50–54]. We provide a comprehensive summary of all tested systematic uncertainties in the Supplemental Material.

The limits derived in this work are compared to other limits and sensitivities of future experiments in Fig. 2 (right). Our results give the strongest constraints to date for $0.5 \lesssim m_{a,\mathrm{neV}} \lesssim 20$ and surpass the expected limits for the planned ALPS II experiment [55] in that range. They are only a factor of ~ 2 below the exclusion prospects of the planned IAXO experiment [56]. We note that the systematic uncertainties of the future experiments are likely to be smaller than the ones that apply to the present analysis. In conjunction with other limits taken at face value [25, 39, 49], the parameter space where ALPs could explain hints for a lower γ-ray opacity compared to EBL-model predictions (light blue region, [21]) is now strongly constrained. The limits do not constrain ALPs that could make up the entire DM content of the Universe. This corresponds to the region in Fig. 2 (right) below the $\theta_1 \mathcal{N} = 1$ line, where $\mathcal{N}$ is a model dependent factor and θ_1 is the misalignment angle [9]. Our analysis only constrains ALPs that make up less than $4\,\%$ of the DM, or equivalently $\theta_1 \mathcal{N} > 5$.

308   Observations with future γ-ray instruments could improve the reported limits and test
309 ALP DM models. The planned Gamma-400 satellite, with an envisaged energy resolution
310 of $1\,\%$ above $10\,\mathrm{GeV}$ [57], might be able to better resolve the spectra and probe higher ALP
311 masses. Higher masses could also be reached with the future Cherenkov Telescope Array
312 (CTA) [58].

313   It will be possible to reduce the uncertainties of the intra-cluster B field with the upcoming
314 Square Kilometer Array (SKA) that will conduct a full-sky polarisation survey [59]. It is
315 expected that SKA will observe hundreds of RMs of background sources for the most massive
316 clusters, thereby enabling a more precise determination of their magnetic fields [60].

317   The analysis presented here can be easily extended to other sources that reside in clusters
318 (e.g. M 87 in the Virgo cluster) or in general to any source where ALP-induced spectral
319 irregularities are expected. ALP parameters not constrained in the present analysis (such
320 as those of the "hole"-like feature) could be probed with the different B-field configurations
321 in other sources.
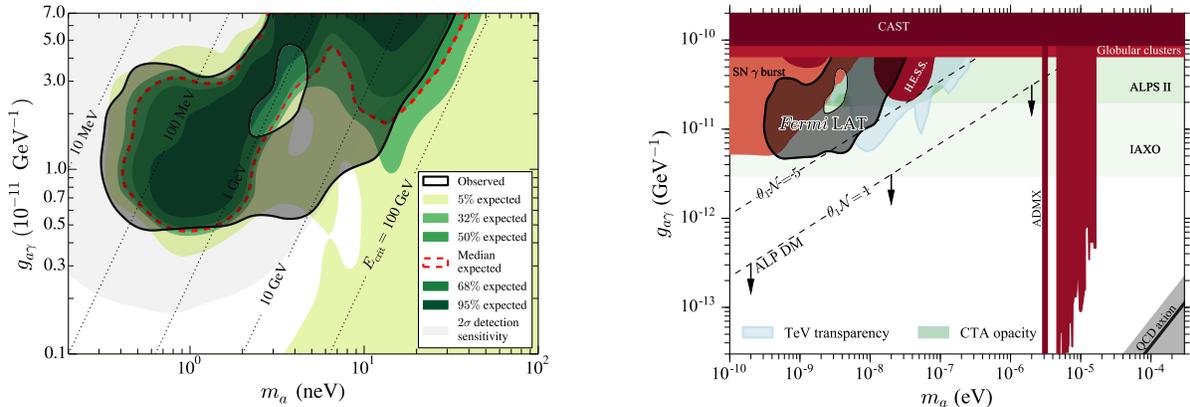
FIG. 2. *Left*: Observed and expected $95\,\%$ confidence limits on the ALP parameters from 400
Monte-Carlo simulations. Dotted lines correspond to constant critical energies. The hatched
gray region shows the parameters where ALPs are detectable at the $2\,\sigma$ confidence level (median
sensitivity). *Right*: Comparison of *Fermi*-LAT limits with other works. Other Limits are shown
in red, expected sensitivities in green. The parameter space where ALPs could explain a low γ-ray
opacity is shown in blue. ALPs below the $\mathcal{N}\theta_1 = 1$ line could account for all the DM. The QCD
axion is shown as a gray shaded band and solid black line. See, e.g. [61] and references therein.

————

* conrad@fysik.su.se

† manuel.meyer@fysik.su.se

‡ sanchezconde@fysik.su.se

[1] J. Jaeckel and A. Ringwald, Annual Review of Nuclear and Particle Science **60**, 405 (2010), arXiv:1002.0329 [hep-ph].

[2] R. D. Peccei and H. R. Quinn, Physical Review Letters **38**, 1440 (1977).

[3] S. Weinberg, Physical Review Letters **40**, 223 (1978).

[4] F. Wilczek, Physical Review Letters **40**, 279 (1978).

[5] E. Witten, Physics Letters B **149**, 351 (1984).

[6] A. Ringwald, Journal of Physics Conference Series **485**, 012013 (2014).

[7] J. Preskill, M. B. Wise, and F. Wilczek, Physics Letters B **120**, 127 (1983).

[8] D. J. E. Marsh, Phys. Rev. D **83**, 123526 (2011), arXiv:1102.4851 [astro-ph.CO].

[9] P. Arias, D. Cadamuro, M. Goodsell, J. Jaeckel, J. Redondo, and A. Ringwald, JCAP **6**, 013 (2012), arXiv:1201.5902 [hep-ph].

[10] G. Raffelt and L. Stodolsky, Phys. Rev. D **37**, 1237 (1988).

[11] K. A. Hochmuth and G. Sigl, Phys. Rev. D **76**, 123011 (2007), arXiv:0708.1144.

[12] A. de Angelis, O. Mansutti, and M. Roncadelli, Physics Letters B **659**, 847 (2008), arXiv:0707.2695.

[13] D. Wouters and P. Brun, Phys. Rev. D **86**, 043005 (2012), arXiv:1205.6428 [astro-ph.HE].

[14] A. de Angelis, M. Roncadelli, and O. Mansutti, Phys. Rev. D **76**, 121301 (2007), arXiv:0707.4312.

14

[15] A. De Angelis, O. Mansutti, M. Persic, and M. Roncadelli, MNRAS **394**, L21 (2009), arXiv:0807.4246.

[16] A. de Angelis, G. Galanti, and M. Roncadelli, Phys. Rev. D **84**, 105030 (2011), arXiv:1106.1132 [astro-ph.HE].

[17] D. Horns and M. Meyer, JCAP **2**, 033 (2012), arXiv:1201.4711 [astro-ph.CO].

[18] G. Rubtsov and S. Troitsky, JETP Lett. **100**, 397 (2014), arXiv:1406.0239 [astro-ph.HE].

[19] M. A. Sánchez-Conde, D. Paneque, E. Bloom, *et al.*, Phys. Rev. D **79**, 123511 (2009), arXiv:0905.3270 [astro-ph.CO].

[20] A. Domínguez, M. A. Sánchez-Conde, and F. Prada, JCAP **11**, 020 (2011), arXiv:1106.1860 [astro-ph.CO].

[21] M. Meyer, D. Horns, and M. Raue, Phys. Rev. D **87**, 035027 (2013), arXiv:1302.1208 [astro-ph.HE].

[22] G. Galanti, M. Roncadelli, A. De Angelis, and G. F. Bignami, ArXiv e-prints (2015), arXiv:1503.04436 [astro-ph.HE].

[23] J. Biteau and D. A. Williams, ArXiv e-prints (2015), arXiv:1502.04166.

[24] A. Domínguez and M. Ajello, ApJ **813**, L34 (2015), arXiv:1510.07913 [astro-ph.HE].

[25] A. Abramowski, F. Acero, F. Aharonian, *et al.* (H.E.S.S. Collaboration), Phys. Rev. D **88**, 102003 (2013), arXiv:1311.3148 [astro-ph.HE].

[26] M. Ackermann *et al.* (*Fermi*-LAT Collaboration), Astrophys. J. **810**, 14 (2015), arXiv:1501.06054 [astro-ph.HE].

[27] See Supplemental Material, which includes Refs. [62-72].

[28] J. Aleksić *et al.* (MAGIC Collaboration), A&A **564**, A5 (2014), arXiv:1310.8500 [astro-ph.HE].

[29] F. Tavecchio and G. Ghisellini, MNRAS **443**, 1224 (2014), arXiv:1404.6894 [astro-ph.HE].

[30] G. B. Taylor, N. E. Gugliucci, A. C. Fabian, *et al.*, MNRAS **368**, 1500 (2006), astro-ph/0602622.

[31] W. Atwood, A. Albert, L. Baldini, *et al.*, ArXiv e-prints (2013), arXiv:1303.3514 [astro-ph.IM].

[32] M. Ackermann *et al.* (*Fermi*-LAT Collaboration), Accepted for publication in ApJS (2015), arXiv:1508.04449 [astro-ph.HE].

[33] C. Csáki, N. Kaloper, M. Peloso, and J. Terning, JCAP **5**, 005 (2003), hep-ph/0302030.

[34] M. Meyer, D. Montanino, and J. Conrad, JCAP **9**, 003 (2014), arXiv:1406.5972 [astro-ph.HE].

15

[35] D. Hooper and S. Profumo, Phys. Rep. **453**, 29 (2007), arXiv:hep-ph/0701197.

[36] R. Jansson and G. R. Farrar, ApJ **757**, 14 (2012), arXiv:1204.3662 [astro-ph.GA].

[37] A. Domínguez, J. R. Primack, D. J. Rosario, *et al.*, MNRAS **410**, 2556 (2011), arXiv:1007.1459 [astro-ph.CO].

[38] A. Ayala, I. Domínguez, M. Giannotti, *et al.*, Phys. Rev. Lett. **113**, 191302 (2014), arXiv:1406.6053 [astro-ph.SR].

[39] A. Payez, C. Evoli, T. Fischer, *et al.*, JCAP **2**, 006 (2015), arXiv:1410.3747 [astro-ph.HE].

[40] K. Dolag, A. M. Bykov, and A. Diaferio, Space Sci. Rev. **134**, 311 (2008), arXiv:0801.1048.

[41] Y. Dubois and R. Teyssier, A&A **482**, L13 (2008), arXiv:0802.0490.

[42] L. Feretti, G. Giovannini, F. Govoni, and M. Murgia, A&A Rev. **20**, 54 (2012), arXiv:1205.1919 [astro-ph.CO].

[43] E. Churazov, W. Forman, C. Jones, and H. Böhringer, ApJ **590**, 225 (2003), astro-ph/0301482.

[44] J. Aleksić, E. A. Alvarez, L. A. Antonelli, *et al.* (MAGIC Collaboration), A&A arXiv:1111.5544.

[45] P. Kuchar and T. A. Enßlin, A&A **529**, A13 (2011).

[46] V. Vacca, M. Murgia, F. Govoni, L. Feretti, G. Giovannini, R. A. Perley, and G. B. Taylor, A&A **540**, A38 (2012), arXiv:1201.4119 [astro-ph.CO].

[47] M. Ackermann *et al.* (*Fermi*-LAT Collaboration), Phys. Rev. D **89**, 042001 (2014).

[48] M. Ackermann *et al.* (*Fermi*-LAT Collaboration), accepted for publication in Phys. Rev. Lett. (2015), arXiv:1503.02641 [astro-ph.HE].

[49] D. Wouters and P. Brun, ApJ **772**, 44 (2013), arXiv:1304.0989 [astro-ph.HE].

[50] A. Franceschini, G. Rodighiero, and M. Vaccari, A&A **487**, 837 (2008), arXiv:0805.1841.

[51] J. D. Finke, S. Razzaque, and C. D. Dermer, ApJ **712**, 238 (2010), arXiv:0905.1115 [astro-ph.HE].

[52] T. M. Kneiske and H. Dole, A&A **515**, A19+ (2010), arXiv:1001.2132 [astro-ph.CO].

[53] R. C. Gilmore, R. S. Somerville, J. R. Primack, and A. Domínguez, MNRAS **422**, 3189 (2012), arXiv:1104.0671 [astro-ph.CO].

[54] Y. Inoue, S. Inoue, M. A. R. Kobayashi, R. Makiya, Y. Niino, and T. Totani, ApJ **768**, 197 (2013), arXiv:1212.1683.

[55] R. Bähre, B. Döbrich, J. Dreyling-Eschweiler, *et al.*, Journal of Instrumentation **8**, T09001

(2013), arXiv:1302.5647 [physics.ins-det].

[56] I. G. Irastorza, F. T. Avignone, G. Cantatore, *et al.*, Journal of Physics Conference Series **460**, 012002 (2013).

[57] P. Cumani, A. M. Galper, V. Bonvicini, *et al.*, ArXiv e-prints (2015), arXiv:1502.02976 [astro-ph.IM].

[58] M. Actis, G. Agnetta, F. Aharonian, *et al.* (CTA Consortium), Experimental Astronomy **32**, 193 (2011), arXiv:1008.3703 [astro-ph.IM].

[59] B. M. Gaensler, R. Beck, and L. Feretti, New Astronomy Reviews **48**, 1003 (2004), astro-ph/0409100.

[60] A. Bonafede, F. Vazza, M. Brggen, T. Akahori, E. Carretti, *et al.*, PoS **AASKA14**, 095 (2015), arXiv:1501.00321 [astro-ph.CO].

[61] M. Meyer and J. Conrad, JCAP **12**, 016 (2014), arXiv:1410.1556 [astro-ph.HE].

[62] M. Ackermann *et al.* (Fermi-LAT Collaboration), Astrophys.J.Suppl. **203**, 4 (2012), arXiv:1206.1896 [astro-ph.IM].

[63] A. Mirizzi and D. Montanino, JCAP **12**, 4 (2009), arXiv:0911.0015 [astro-ph.HE].

[64] A. Mirizzi, G. G. Raffelt, and P. D. Serpico, Phys. Rev. D **76**, 023001 (2007), arXiv:0704.3044.

[65] A. Dobrynina, A. Kartavtsev, and G. Raffelt, Phys. Rev. D **91**, 083003 (2015), arXiv:1412.4777 [astro-ph.HE].

[66] D. Horns, L. Maccione, M. Meyer, A. Mirizzi, D. Montanino, and M. Roncadelli, Phys. Rev. D **86**, 075024 (2012), arXiv:1207.0776 [astro-ph.HE].

[67] N. Bassan, A. Mirizzi, and M. Roncadelli, JCAP **5**, 010 (2010), arXiv:1001.5267 [astro-ph.HE].

[68] S. S. Wilks, Annals of Mathematical Statistics **9**, 60 (1938).

[69] G. Cowan, K. Cranmer, E. Gross, and O. Vitells, European Physical Journal C **71**, 1554 (2011), arXiv:1007.1727 [physics.data-an].

[70] M. Ackermann *et al.* (*Fermi*-LAT Collaboration), Phys. Rev. **D91**, 122002 (2015), arXiv:1506.00013 [astro-ph.HE].

[71] A. Albert, G. A. Gómez-Vargas, M. Grefe, C. Muñoz, C. Weniger, E. D. Bloom, E. Charles, M. N. Mazziotta, and A. Morselli, JCAP **10**, 023 (2014), arXiv:1406.3430 [astro-ph.HE].

[72] A. Bonafede, L. Feretti, M. Murgia, F. Govoni, G. Giovannini, D. Dallacasa, K. Dolag, and G. B. Taylor, A&A **513**, A30 (2010), arXiv:1002.0594 [astro-ph.CO] .